A Submersible Autonomous Sensor for Spectrophotometric pH Measurements of Natural Waters

ARTICLE *in* ANALYTICAL CHEMISTRY · MAY 2003

Impact Factor: 5.64 · DOI: 10.1021/ac020568l · Source: PubMed

4 AUTHORS, INCLUDING:

Mike DeGrandpre
University of Montana

84 PUBLICATIONS **1,949** CITATIONS

SEE PROFILE

Anal. Chem. **2003,** *75,* 1844−1850

A Submersible Autonomous Sensor for Spectrophotometric pH Measurements of Natural Waters

Todd R. Martz, Jeffrey J. Carr, Craig R. French, and Michael D. DeGrandpre*

Department of Chemistry, The University of Montana, Missoula, Montana 59812

An autonomous sensor for long-term in situ measurements of the pH of natural waters is described. The system is based upon spectrophotometric measurements of a mixture of sample and sulfonephthalein indicator. A simple plumbing design, using a small, low-power solenoid pump and valve, avoids the need for quantitative addition of indicator. A ∼50-μL slug of indicator is pulled into the sample stream by the pump, and subsequent pumping and mixing results in a section of indicator and sample where absorbance measurements can be made. The design also permits direct determination of the indicator pH perturbation. Absorbances are recorded at three wavelengths (439, 579, and 735 nm) using a custom-built 1.7-cm path length fiber-optic flow cell. Solution blanks are obtained by periodically flushing the cell with sample. Field tests were performed in a local river over an 8-day period. The in situ accuracy, based on comparison with laboratory spectrophotometric pH measurements, was −0.003 pH unit (n = 16), similar to the measurement precision. No drift was observed during the 8-day period. The absorbance ratio used to calculate pH, in combination with a simple and robust optical design, imparts an inherent stability not achievable with conventional potentiometric methods, making the design feasible for long-term autonomous pH measurements.

The title "master variable" has been given to pH due to its importance in aquatic ecosystems. Determination of pH is critical in understanding the acid−base equilibria of aqueous species such as CO_2 and NH_3.[1] Trace metal solubility and speciation, and consequently metal mobilization, are also highly pH dependent.[1,2] Models of aqueous systems must consider pH when choosing between a thermodynamic or kinetic pathway.[3] High-precision monitoring of pH has been used in both seawater[4] and freshwater[5] as an indicator of biological production and respiration. Long-term measurements of pH can serve as an early warning sign of lake acidification.[6,7] These studies are just a few examples of the many applications of pH in aquatic sciences.

There is a need for more autonomous chemical sensors in environmental research and monitoring. Studies based upon periodic sampling may miss episodic events and are not able to resolve short-term variations for extended periods. In the case of pH, sampling may also compromise data quality due to gas exchange or biological alteration during storage (i.e., CO_2 loss or gain). Autonomous in situ pH instrumentation can provide more extensive, and perhaps more reliable, data for characterizing biogeochemical dynamics in aquatic systems. There has accordingly been a substantial effort to develop robust autonomous pH-sensing systems. Many in situ systems are commercially available (e.g., Sea Bird Electronics Inc., YSI Inc., In Situ Inc., Analytical Sensors Inc.), and independent researchers[5,8,9] as well as government agencies (e.g., United States Geological Survey) often use custom-designed instruments. All of these systems utilize potentiometric glass pH electrodes.

Although popular because of their simplicity and low cost, glass pH electrodes have several shortcomings for autonomous sensing in natural waters, especially low ionic strength and poorly buffered waters. The primary problems arise from irreproducible junction potentials and junction potential drift[10] encountered in both seawater[11] and freshwater.[12] Interlaboratory standard protocols have proven difficult to implement, and none are collectively accepted and used by the scientific community.[13] Even when calibrated frequently, large systematic errors can arise from differences between standard and sample junction potentials. For example, an in situ dual-electrode instrument produced systematic errors of 0.1 pH unit between the two electrodes[5] and Robowell, a newly developed USGS remote sensor, exhibits offsets as high as 0.5 pH unit.[14] Although autonomous electrode-based studies have provided a wealth of valuable information, improved methods

* Corresponding author. E-mail: mdegrand@selway.umt.edu.

(1) Stumm, W.; Morgan, J. J. *Aquatic Chemistry: Chemical Equilibria and Rates In Natural Waters*, 3rd ed.; John Wiley & Sons: New York, 1996; Chapters 3−5, 10.
(2) Borg, H.; Ek, J.; Holm, K. *Water, Air, Soil Pollut.* **2001**, *130*, 1757−1762.
(3) Pankow, J. F.; Morgan, J. J. *Environ. Sci. Technol.* **1981**, *15*, 1306−1313.
(4) Furhmann, R.; Zirino, A. *Deep-Sea Res.* **1988**, *35*, 197−208.
(5) Maberly, S. C. *Freshwater Biol.* **1996**, *35*, 579−598.
(6) Henriksen, A. *Nature* **1979**, *278*, 542−545.
(7) Heonicke, R.; Stapanian, M. A.; Arnet, L. J.; Metcalf, R. C. *Freshwater Biol.* **1991**, *25*, 261−278.
(8) Cai, W.; Reimers, C. E. *Limnol. Oceanogr.* **1993**, *38*, 1762−1773.
(9) Le Bris, N.; Sarradin, P. M.; Pennec, S. *Deep-Sea Res. I* **2001**, *48*, 1941−1951.
(10) Brezinski, D. P. *Analyst* **1983**, *108*, 425−442.
(11) Dickson, A. G. *Mar. Chem.* **1993**, *44*, 131−142.
(12) Davison, W.; Woof, C. *Anal. Chem.* **1985**, *57*, 2567−2570.
(13) Gardner, M. J.; Gill, R.; Ravenscroft, J. E. *Analyst* **1990**, *115*, 371−374.
(14) Granato, G. E.; Smith, K. P. *Groundwater Monit. Remediat.* **1999**, *19*, 81−89.

10.1021/ac020568l CCC: $25.00
Published on Web 03/06/2003

are needed to address contemporary geochemical and environmental monitoring problems.

Spectrophotometric determination of pH using sulfonephthalein indicators is one option that offers many advantages over potentiometry.[15,16] Unlike electrodes, which would not typically output the same potential for the same solution, good quality spectrophotometers will output the same absorbance value. This inherent reproducibility has made spectrophotometric pH appealing for oceanographic research where long-term reproducibility is critical.[17−20] Spectrophotometric pH measurements of seawater regularly achieve a precision of ±0.0004 pH unit[16] and an accuracy of ±0.001 pH unit.[21] The spectrophotometric pH method has also recently been revisited for freshwater applications.[22,23]

While a number of automated spectrophotometric pH analyzers have been designed for shipboard measurements,[24,25] few have been sufficiently simple to adapt to an autonomous in situ system. A spectrophotometric pH sensor has recently been designed for moored platforms and has been successfully deployed in the North Pacific for a 1-month period.[26] In the present article, we describe an autonomous spectrophotometric pH sensor developed by simple modifications of our submersible autonomous moored instrument for CO_2 (SAMI-CO_2),[27] a partial pressure of carbon dioxide (pCO_2) sensor. We have named the new sensor SAMI-pH because of its close relationship with the SAMI-CO_2.

Operating Principle Overview. For a detailed review of spectrophotometric pH measurements, see Clayton and Byrne.[16] For freshwater specifically, see Yao and Byrne[22] and French et al.[23] In brief, the method is based upon the equilibrium of a weak acid pH indicator:

$$HL^- \overset{K_a}{\rightleftharpoons} H^+ + L^{2-} \qquad (1)$$

where HL^- is the monoprotic form of the indicator and L^{2-} is the deprotonated form (the diprotic form is completely dissociated at typical freshwater and marine pH). Spectrophotometric pH is calculated with

$$pH = pK_a' + \log\left(\frac{R - e_1}{e_2 - Re_3}\right) \qquad (2)$$

where pK_a' is the negative log of the apparent dissociation constant, R is A_2/A_1 where A_1 and A_2 are absorbances at HL^- and L^{2-} peak wavelengths λ_1 and λ_2, respectively, and the e_i's are ratios of the molar absorptivities (ϵ) corresponding to the HL^- or L^{2-} form (denoted by a or b, respectively) at λ_1 or λ_2,

$$e_1 = \frac{{}^a\epsilon_{\lambda_2}}{{}^a\epsilon_{\lambda_1}} \qquad e_2 = \frac{{}^b\epsilon_{\lambda_2}}{{}^a\epsilon_{\lambda_1}} \qquad e_3 = \frac{{}^b\epsilon_{\lambda_1}}{{}^a\epsilon_{\lambda_1}}. \qquad (3)$$

Cresol red (CR, $pK_a' \sim 8.29$ at 20 °C and 0.01 M ionic strength) was selected for this study to match the pH of a local river (the Clark Fork) where we have recently undertaken field studies.[23,28] The temperature-dependent pK_a' and e_i's are taken from French et al.[23] The analytical wavelengths selected for CR are 439 (λ_1) and 579 nm (λ_2).

A spectrophotometric pH measurement requires addition of a small amount of indicator to the sample.[15,16] The weak acid indicator can perturb the sample pH, especially the pH of poorly buffered freshwater samples.[23] For this reason, a cuvette with a 10-cm path length is often used to minimize the amount of indicator added. In addition, an exact amount is pipeted into the sample to ensure that the perturbation is reproducible. Automated spectrophotometric pH methods use a high-precision peristaltic pump[24,25] or syringe pump[29] to inject a reproducible amount of indicator into a sample stream. While appropriate for shipboard analyzers, the complexity, power consumption, and other limitations of automated pipets (or burets) and peristaltic pumps make them unattractive for long-term deployments. The system described here uses a very simple pump and plumbing design, better suited for autonomous in situ measurements. During a SAMI-pH measurement cycle, a solenoid pump pulls a slug of indicator into the sample stream. Subsequent pumping and mixing provides a section of indicator and sample where absorbance measurements can be made. Collection of absorbance data over a range of indicator concentration also allows for direct correction of the pH perturbation. The specific configuration and components of the SAMI-pH are described below.

EXPERIMENTAL SECTION

General Instrument Design. As stated above, the SAMI-pH (Figure 1) is based on simple modifications to the SAMI-CO_2.[27,30] To perform pH measurements, the SAMI-CO_2 design is altered as follows (refer to Figure 1): (a) the normally open (NO) valve port is connected to a natural water sample in place of a bromothymol blue indicator solution, (b) the normally closed (NC) valve port is connected to the CR indicator solution (2.00×10^{-2} mol kg^{-1} CR) in place of a deionized water blank, (c) a mixing coil replaces a gas-permeable membrane, (d) the flow cell path length is increased, and (e) detection wavelengths are changed to suit CR.

(15) Byrne, R. H.; Breland, J. A. *Deep-Sea Res.* **1989**, *36*, 803−810.
(16) Clayton, T. D.; Byrne, R. H. *Deep-Sea Res.* **1993**, *40*, 2115−2129.
(17) King, D. W.; Kester, D. R. *Mar. Chem.* **1989**, *26*, 5−20.
(18) Byrne, R. H.; McElligott, S.; Feely, R. A.; Millero, F. J. *Deep-Sea Res.* **1999**, *46*, 1985−1997.
(19) Bellerby, R. G. J.; Olsen, A.; Johannessen, T.; Croot, P. *Talanta* **2002**, *56*, 61−69.
(20) Lamb, M. F.; Sabine, C. L.; Feely, R. A.; Wanninkhof, R.; Key, R. M.; Johnson, G. C.; Millero, F. J.; Lee, K.; Peng, T. H.; Kozyr, A.; Bullister, J. L.; Greeley, D.; Byrne, R. H.; Chipman, D. W.; Dickson, A. G.; Goyet, C.; Guenther, P. R.; Ishii, M.; Johnson, K. M.; Keeling, C. D.; Ono, T.; Shitashima, K.; Tilbrook, B.; Takahashi, T.; Wallace, D. W. R.; Watanabe, Y. W.; Winn, C.; Wong, C. S. *Deep-Sea Res. II* **2002**, *49*, 21−58.
(21) Millero, F. J.; Zhang, J.; Fiol, S.; Sotolongo, S.; Roy, R. N.; Lee, K.; Mane, S. *Mar. Chem.* **1993**, *44*, 143−152.
(22) Yao, W.; Byrne, R. H. *Environ. Sci. Technol.* **2001**, *35*, 1197−1201.
(23) French, C. R.; Carr, J. J.; Dougherty, E. M.; Eidson, L. A. K.; Reynolds, J. C.; DeGrandpre, M. D. *Anal. Chim. Acta* **2002**, *453*, 13−20.
(24) Bellerby, R. G. J.; Turner, D. R.; Millward, G. E.; Worsfold, P. J. *Anal. Chim. Acta* **1995**, *309*, 259−270.
(25) Tapp, M.; Hunter, K.; Currie, K.; Mackaskill, B. *Mar. Chem.* **2000**, *72*, 193−202.
(26) Kaltenbacher, E.; Steimle, E. T.; Byrne, R. H. *Proc. 2000 Int. Symp. Underwater Technol.* **2000**, *IEEE00EX418*, 41−45.
(27) DeGrandpre, M. D.; Hammar, T. R.; Smith, S. P.; Sayles, F. L. *Limnol. Oceanogr.* **1995**, *40*, 969−975.
(28) Reynolds, J. C. M.S. Thesis, The University of Montana, Missoula, MT, 2001.
(29) DelValls, T. A. *Cienc. Mar.* **1999**, *25*, 345−365.
(30) DeGrandpre, M. D.; Baehr, M. M.; Hammar, T. R. *Anal. Chem.* **1999**, *71*, 1152−1159.

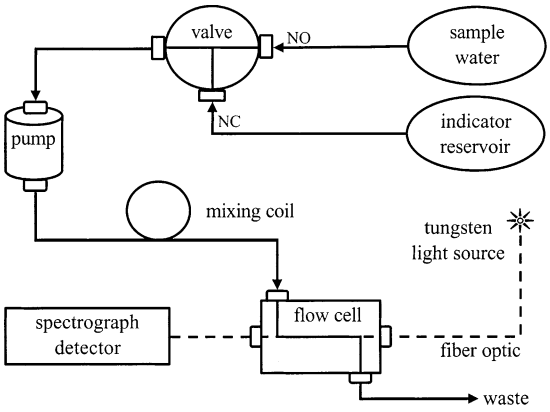

Figure 1. Schematic layout of the submersible autonomous moored instrument for pH (SAMI-pH). SAMI-pH was created through simple modifications of a system used to measure the partial pressure of CO_2 (SAMI-CO_2).[27,30] Valve settings are normally open (NO) and normally closed (NC).

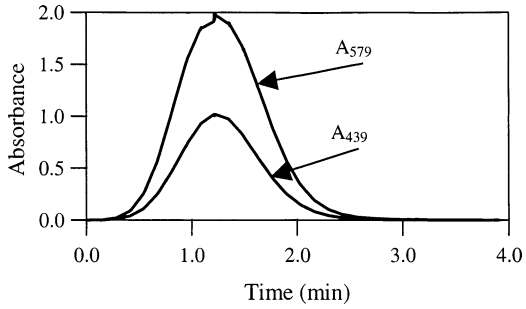

Figure 2. Absorbances of an indicator pulse as it passes through the fiber-optic flow cell. The sample pH and indicator pH perturbation are derived using data at the dilute tail edge of the peak (Figure 3). Slight jumps in absorbance are caused by variable flow from the solenoid (pulse) pump.

Following Figure 1, a SAMI-pH measurement is made by switching the valve to NC and activating the pump to pull a slug of indicator into the flow line. The indicator slug is followed by pulses of sample water (valve is switched to NO), which drive the indicator toward the mixing coil and optical flow cell. Mixing occurs at both the front and tail ends of the indicator peak, providing two sections over which appropriate absorbances can be recorded (Figure 2). In the present design, the SAMI-pH is programmed to acquire data on the tail end of the indicator pulse (Figures 2 and 3). The indicator pH perturbation can be clearly seen by plotting the calculated pH over the total indicator concentration ($[CR]_T$) range found at the tail end of the peak (Figure 3B and C). To derive Figure 3B, $[CR]_T$ was calculated by first assuming A_{579} was due solely to L^{2-} (i.e., $e_1 = 0$) and using Beer's law to solve directly for $[L^{2-}]$. $[HL^-]$ can then be found from eq 2, and $[CR]_T$ can be calculated. Note that because the indicator pH is less than the sample pH, the calculated pH increases as $[CR]_T$ approaches zero (Figure 3C). Data such as these can be used to correct for the pH perturbation, as described in more detail below.

Flow Components. A three-way solenoid valve (model 2535043, Neptune Research Corp.) is used to switch between the water sample and indicator reservoir (Figure 1). Fluid is pumped using a 50 μL per pulse solenoid pump (LPLA1210050L, The Lee Co.). The mixing coil consists of a 24-cm length of 0.10-cm-i.d. PEEK tubing (Upchurch Corp.). A gas-impermeable reagent bag (Pollution Measurement Corp.) is filled with 2.00×10^{-2} mol kg^{-1} CR and enclosed in a PVC box attached to the side of the main housing. A short length of 0.10-cm-i.d. PEEK tubing serves as the water inlet. The flow rate, controlled by back pressure from a 13.5-cm length of 0.10-cm-i.d. PEEK tubing placed at the optical cell outlet, is ~14 μL s^{-1}. A single measurement requires 50 μL of indicator (1 pump pulse) and 1.6 mL of sample (32 pulses).

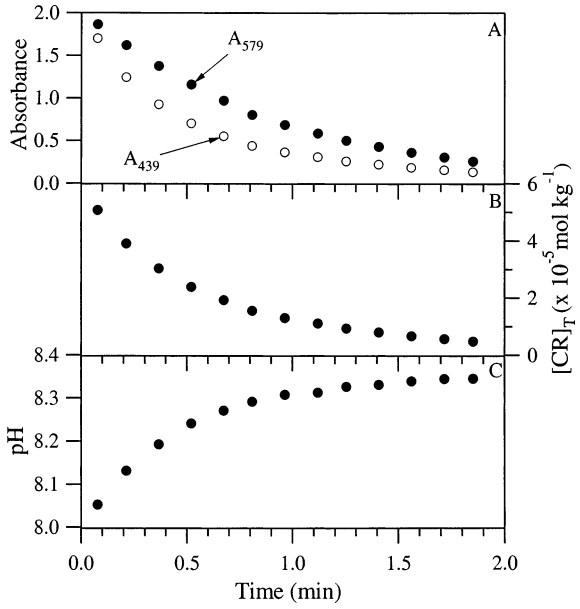

Figure 3. Typical data collected from the tail end of an indicator pulse (Figure 2) for a single pH measurement: the indicator absorbances (A), total indicator concentration ($[CR]_T$) (B), and calculated pH (C). The change in measured pH along the indicator profile is due to perturbation of the sample pH by the indicator. Data in (B) and (C) can be used to directly determine the indicator pH perturbation (Figure 5). Each point corresponds to one pump pulse.

Optical Design. Optical measurements are made using a miniature, single-beam spectrophotometric detection system. The output from a low-power tungsten lamp (5 V, 0.12 A, Gilway Technical Lamps) is coupled to a 600-μm core fused-silica fiber optic (F-MSC-OPT, Newport Corp.). The fiber optic carries the light to an ultra-high-density polyethylene optical flow cell.[27] The flow cell optical channel is 1.72 cm long with a 610-μm i.d. Because no collimating optics are used in the SAMI design, light throughput drops precipitously with path lengths longer than ~1.7 cm. Light transmitted through the cell is carried by a second 600-μm core fiber optic to a grating spectrograph (f/2.5, R_d = 10 nm mm^{-1}) (MS10, American Holographic). Three 2.4-mm-wide photodiodes are positioned in the focal plane of the spectrograph with spacings that correspond to the analytical wavelengths (439, 579, and 735 nm). Two different photodiodes are used: an IR-insensitive GaP photodiode at 439 nm (G1962, Hamamatsu Corp.) and Si photodiodes at 579 and 735 nm (S2386, Hamamatsu Corp.). Although the CR absorbance maximums are at 434 and 573 nm, we chose 439 and 579 nm because of the availability of optical interference filters at these wavelengths (used to position the spectrograph wavelength; see below). The 735-nm detector functions as a reference channel as described in the Absorbance Measurements section. The large surface area photodiodes are required to obtain sufficient signal-to-noise ratio but result in a relatively large (±12 nm) spectral band-pass, which has important

consequences, as discussed below. Detector current is converted to voltage and then stored using a low-power data logger (Tattletale 4A, Onset Computer Corp.). A more detailed description of the optical flow cell design and detection system may be found in DeGrandpre et al.[27,30]

Accurate spectrophotometric pH measurements require accurate knowledge of the peak wavelength and spectral band-pass. Both of these parameters must be consistent with those used for the molar absorptivity ratios (eq 3) to avoid creating significant systematic pH errors (eq 2). The e_i's are typically determined on a benchtop UV−visible spectrophotometer with a narrow band-pass (e.g., ±2 nm).[16] To obtain e_i's consistent with SAMI-pH absorbance values (i.e., calculated from the intensity measured over a ±12-nm band-pass), the UV−visible absorbances used to derive the e_i's must be converted to intensities, averaged over each ±12-nm band-pass and converted back to absorbance. Because the large band-pass spans a large range of molar absorptivities (the CR spectrum is shown in French et al.[23]), the SAMI-pH is very sensitive to wavelength accuracy. For example, a ±2-nm wavelength error at 579 nm results in a ±0.04 pH error. The spectrograph wavelengths are verified in the laboratory using commercially available narrow band-pass interference filters. The interference filter peak transmittance wavelengths were confirmed to within ±0.2 nm using a benchtop UV−visible spectrophotometer. Prior studies have shown that the spectrograph wavelength calibration is stable over a wide range of environmental conditions.[27,30]

Absorbance Measurements. Any absorbance-based measurement requires blank readings before absorbance can be calculated. A blank measurement is obtained in the SAMI-pH by completely flushing the system with sample and recording intensities at all three wavelengths. These intensities are used to determine the blank constants (K_λ's):

$$K_{439} = I_{o439}/I_{o735} \quad \text{and} \quad K_{579} = I_{o579}/I_{o735} \qquad (4)$$

where I_{o439}, I_{o579}, and I_{o735} are the intensities at 439, 579, and 735 nm, respectively. Optical absorbances are then calculated using[27]

$$A_\lambda = -\log(I_\lambda/I_{ref}K_\lambda) \qquad (5)$$

where A_λ is the sample absorbance at 439 or 579 nm, I_λ is the intensity transmitted through the indicator and sample mixture, K_λ is the blank constant for the most recent blank measurement cycle (eq 4), and I_{ref} is the transmitted intensity at 735 nm, where the indicator does not absorb. The periodic blank measurements and the reference wavelength (735 nm) both compensate for throughput changes in the optical system. The blank constants, K_{439} and K_{579} in eq 5, correct for wavelength-*dependent* changes (e.g., changes in light source color temperature, absorbance of blank) while I_{ref} corrects for short-term intensity changes (e.g., scattering within cell) for every measurement. Blanks are only obtained every 12 h with the present design because flushing requires significant power and time (~6 min and 100 pump pulses; see Figure 4). Blanks may be required more frequently if the sample background absorbance changes over short time periods. An absorbance precision and long-term stability of ±0.001 absorbance unit (between ~0.20 and 1.20 au) are routinely obtained using absorbances calculated with eq 5. Absorbance accuracy, which is primarily dependent upon stray light in the detection system,[30] is ~±0.003 au based on neutral density filter measurements.

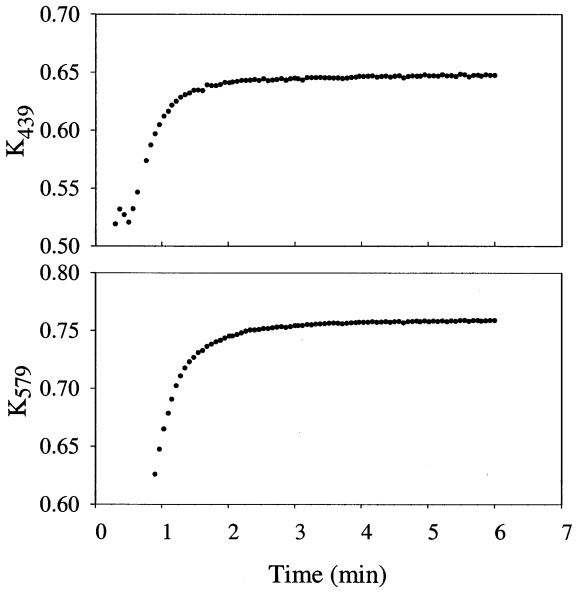

Figure 4. Blank constants, K_{439} (top) and K_{579} (bottom), as indicator is flushed from the flow cell with sample (eq 4). Each point corresponds to a 50-μL pump pulse. One blank requires a sample volume of ~5 mL and ~6 min, after injection of the indicator pulse, for complete flushing.

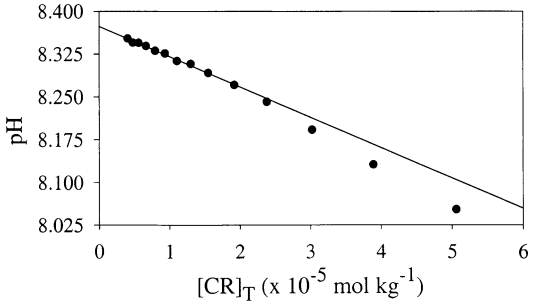

Figure 5. Effect of total indicator concentration, $[CR]_T$, on the measured pH using the data in Figure 3. The least-squares regression through the linear portion of the curve ($[CR]_T < 9.0 \times 10^{-6}$ M) (solid line) is used to determine the unperturbed pH ($[CR]_T = 0$).

Correction for Indicator Perturbation of Sample pH. As presented above, the SAMI-pH design generates data that can be used to directly correct for the pH perturbation (Figure 3). The unperturbed sample pH can be readily found by plotting pH versus $[CR]_T$ and extrapolating to zero indicator concentration (Figure 5). For our purposes, pH versus $[CR]_T$ was not plotted for every measurement because we found in a previous study that the indicator perturbation ($dpH/d[CR]_T$) is nearly constant at the high alkalinities characteristic of the Clark Fork River.[23] However, in less-alkaline, weakly buffered systems the pH perturbation can be determined for every sample using the method shown in Figure 5. It should also be noted that sample dilution by the indicator solution could alter the sample pH. To avoid dilution effects, the indicator is prepared at a sufficiently high concentration so that only small amounts of solution are required to obtain reasonable absorbances. The diluted indicator concentration typically falls within the range 1×10^{-5}–6×10^{-5} mol kg^{-1}, corresponding to

a 1000-fold dilution of the original indicator (Figure 3B). Equilibrium calculations indicate that a 1000-fold sample dilution alters the sample pH by <0.001 pH unit.

Instrument Housing. The electronics and battery pack (16 alkaline C-cells) are contained in a 61-cm length of 15-cm-i.d. PVC pipe with water-tight O-ring seals on both end caps. The top end cap is attached to the internal bracketing, which supports all of the internal components. The pump and valve are located in an external housing (10-cm-long, 5-cm-i.d. PVC pipe) filled with silicon oil and equipped with a rubber diaphragm that equilibrates the internal pressure with ambient hydrostatic pressure. O-ring feedthroughs are used for the fiber optics and electrical connectors. An additional 18-D-cell battery pack is housed in a 50-cm length of 5-cm-i.d. PVC housing.

Testing of SAMI-pH. Laboratory and field SAMI-pH measurements were compared with spectrophotometric pH measurements collected on a double-beam UV−visible spectrophotometer (Cary 300 Bio, Varian Inc.). The spectral band-pass of the UV−visible instrument was set to ±2 nm. A circulating water bath was used to thermostat dual-jacketed 10-cm-path length cells to ±0.1 °C. Samples were analyzed using the following procedure:[23] (1) the sample was placed in a 10-cm cuvette (~25 mL total volume) and brought to the desired temperature, (2) blanks were obtained at 439, 579, and 735 nm, (3) the sample cell was removed; 25 μL of 2.00×10^{-3} mol kg^{-1} CR solution was added and the solution was manually mixed and placed back in the sample compartment, and (4) absorbances were obtained when the desired temperature was reached. The absorbance at 735 nm was used to correct for any baseline offsets caused by removal and replacement of the cell. Three replicate analyses (steps 1−4) were performed on each sample. The average replicate reproducibility was ±0.004 pH unit.

Laboratory evaluation of the SAMI-pH consisted of measurement of a series of buffer solutions.[31] In situ field testing was performed in the Clark Fork River, MT, from October 26, 2000 to November 2, 2000. A stainless steel cage and two cement anchors held the submerged instrument on the river bottom (~1-m depth). The instrument was programmed to measure pH every 15 min. Periodic sampling, with subsequent UV−visible analysis as described above, was used to verify SAMI-pH measurements during deployment. Water samples were obtained at least once per day. Water temperature was measured using a portable electronic temperature probe (Omega HHD, with a reported accuracy of ±0.1 °C). The samples were transported back to the laboratory on ice, where they were immediately analyzed at the measured river temperature. Accuracy, for both laboratory and field testing, is reported relative to the benchtop UV−visible measurements. It is called "relative accuracy" because the absolute accuracy is also dependent upon the accuracy of the indicator pK_a' (eq 2).[16] The uncertainty in the indicator pK_a' at freshwater ionic strengths is discussed in French et al.[23]

RESULTS AND DISCUSSION

Laboratory and Field Results. The SAMI-pH in-laboratory replicate reproducibility is ±0.001 pH ($n = 10$) unit based on repetitive analysis of a boric acid buffer solution (pH = 8.01). The SAMI-pH was also compared to UV−visible measurements over the pH range 7.2−8.8 by using a variety of pH buffers (Table 1). Accuracy and precision both degrade at pH's significantly above and below the indicator pK_a'; however, these measurements include errors for both methods and we were not able to specifically attribute error to either the UV−visible or SAMI-pH. Nonetheless, the data in Table 1 serve to highlight the limited pH range over which indicator-based pH measurements can be accurately made—the usual rule of thumb being ~±1 pH unit around the pK_a'.

Table 1. Mean Error and Standard Deviation of the Error between the SAMI-pH and Benchtop UV−Visible pH Measurements over a Range of pH[a]

pH (UV−vis)	mean error ± 3σ
7.25	0.042 ± 0.035
7.61	−0.010 ± 0.018
7.68	0.003 ± 0.008
8.01	−0.004 ± 0.014
8.32	0.000 ± 0.010
8.50	−0.004 ± 0.021
8.63	−0.012 ± 0.010
8.82	−0.030 ± 0.018

[a] The mean UV−visible pH recorded for the buffers is included for reference. Buffers were prepared from H_3BO_3 and KH_2PO_4. Eight replicates were analyzed at each pH. All measurements were made at 20 °C.

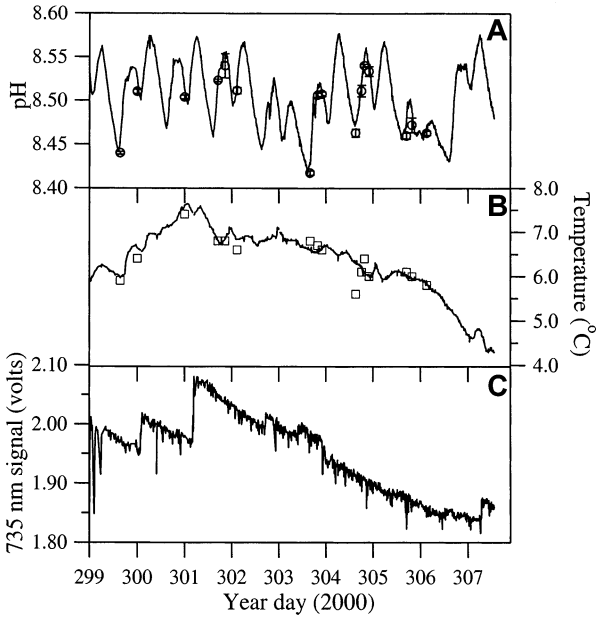

Figure 6. Results from an 8-day deployment in the Clark Fork River, MT, during Fall 2000. SAMI data (A, pH; B, temperature; C, I_{735}) are shown as solid lines and periodic sample pH and temperature as open circles and open squares, respectively. Error bars for the discrete pH data represent ±1σ of the replicate samples ($n = 3$). SAMI and UV−visible data are corrected for the indicator pH perturbation and for differences in measurement temperature.

After the buffer tests verified that the instrument's response was sufficiently accurate and sensitive over the expected pH range of the Clark Fork, we proceeded with field testing. In situ pH and temperature time series during the 8-day deployment period are shown in Figure 6. The SAMI-pH time series resolved the very small diurnal fluctuations during the deployment. Daily changes in pH were less than 0.15 pH unit spanning the range from 8.42

(31) Covington, A. K.; Whalley, P. D.; Davison, W. *Analyst* **1983**, *108*, 1528−1532.

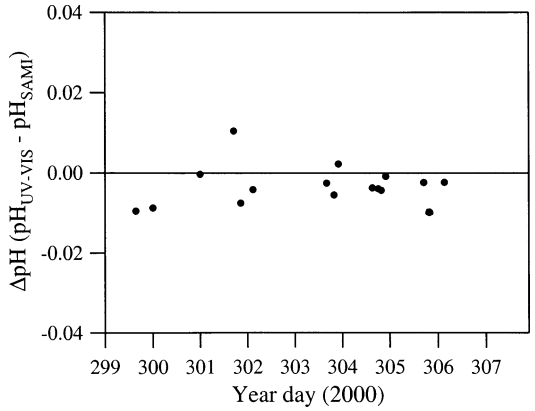

Figure 7. pH difference between discrete samples and SAMI-pH during the 8-day deployment (Figure 6). There is no apparent drift of the in situ instrument over the 8-day deployment period.

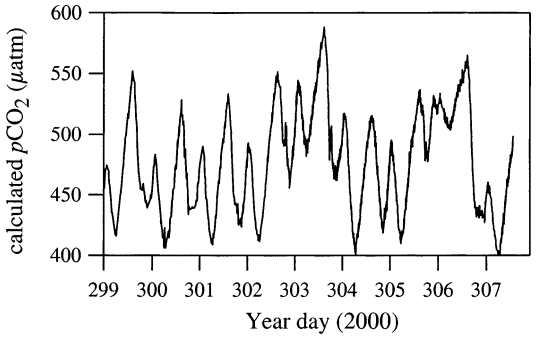

Figure 8. River pCO_2 calculated from the SAMI-pH data shown in Figure 6. Data such as these are used to estimate air−water CO_2 fluxes in aquatic ecosystems. We assumed a constant alkalinity (A_T = 2775 μmol kg^{-1}) (see text for more details).

to 8.57. These changes in pH correspond to absorbance ranges of 0.16 < A_{439} < 0.14 and 0.31 < A_{579} < 0.39.

Prior to comparison of the in situ and sample pH measurements, small corrections had to be made for differences in the measurement conditions. We often found small differences between the SAMI-pH and the UV−visible measurement temperature (averaging ±0.16 °C). The UV−visible pH measurements were corrected to the in situ temperature by determining the sample pH temperature dependence with an in-house CO_2 equilibrium model. The sample pH was calculated for different temperatures using total alkalinity and dissolved inorganic carbon concentrations characteristic of the Clark Fork River (∼2500 μmol kg^{-1}). A linear regression of the pH versus temperature plot gave a slope of 0.014 35 pH unit °C^{-1} which was used to correct the UV−visible measurements to the in situ temperature recorded by the SAMI-pH. Temperature corrections were typically <0.003 pH unit. Both SAMI-pH and UV−visible measurements were also corrected to unperturbed pH's (zero indicator concentration) using the calculated $[CR]_T$ and slope of the line shown in Figure 5. SAMI-pH values were typically corrected by ∼0.03 pH unit while UV−visible values were corrected by ∼0.007 pH unit (less indicator is used in the 10-cm-path length UV−visible measurements).

The resulting relative accuracy of the in situ data was −0.003 ± 0.004 pH unit (n = 16), which is within the precision of the measurement. The SAMI-pH measurements also showed no systematic deviation with time (Figure 7). These results were achieved without use of standards to calibrate the response (i.e., the absorbance ratio, R in eq 2), as required for pH electrodes. The pH resolution obtained during the deployment was better than ±0.005 pH unit. The absorbance resolution required to achieve this pH precision is ∼0.002 and ∼0.003 absorbance unit at the 439- and 579-nm channels, respectively.

The stability and precision of the SAMI-pH is largely due to the use of blank constants and I_{ref} (eqs 4 and 5) that correct for short- and long-term changes in optical throughput as discussed above. The variability in I_{ref} during the deployment is shown in Figure 6C. The large, rapid step changes were caused by movement of the instrument to periodically download data. Other short-term spikes were presumably due to bubbles and particles in the optical path. The slow downward decrease in intensity may have been caused by thermal contraction of the optical cell during the prolonged cooling period (Figure 6B), degradation of the tungsten light source, or an increase in the sample background absorbance. Some wavelength-dependent variability would be expected with this relatively large change in I_{ref} during the deployment. In fact, K_{439} and K_{579} changed by 4.0% and 1.6%, respectively. Errors of ∼0.04 pH unit would have resulted if in situ blank constants were not obtained over the 8-day period. The short-term noise sources are also greatly reduced in the final calculated pH (Figure 6) because of the use of I_{ref} in calculation of the absorbances (eq 5). It should also be noted that the absorbance ratio offers an additional level of noise and drift reduction (e.g., caused by path length fluctuations).

Applications of the SAMI-pH Data. Although the pH changes are small (<0.15), the SAMI-pH data revealed a distinct diurnal cycle (Figure 6A). Our previous studies of the Clark Fork River have found that biological production and respiration create large diurnal pH changes.[28] The "twin peaks" each 24-h period originated from an upstream reservoir with a ∼10-h residence time. The alkaline pH's observed during this study result from groundwater input in addition to net photosynthetic uptake of CO_2. Although the pH data are interesting in their own right, pH can also be used as a master variable for biogeochemical calculations. Others have used similar spatial or temporal pH data to evaluate biological processes in both freshwater[5,32] and seawater.[4,8] Our interests include using pH to calculate the CO_2 speciation in aquatic ecosystems. For example, Figure 8 shows pCO_2 calculated from the SAMI-pH time series in Figure 6 using our in-house CO_2 equilibrium model. The pCO_2 was determined for each SAMI-pH measurement, assuming total alkalinity was constant (A_T = 2775 μmol kg^{-1}). The pCO_2 magnitude and fluctuations in Figure 8 are similar to those observed in previous studies where pCO_2 was measured directly with the SAMI-CO_2.[28] Data such as these can be used to estimate air−sea exchange of CO_2 for global carbon cycle budgets.[33] The pCO_2 calculation is very sensitive to pH errors, however. The ±0.1 unit (∼0.1%) error in pH typical of an electrode results in an uncertainty in the absolute pCO_2 level of ±100 μatm. A 100-μatm offset in pCO_2 would clearly nullify the accuracy of air−water CO_2 flux predictions. Global carbon cycle

(32) Deb, S. C.; Matsushige, K.; Fukushima, T.; Ikei, M.; Ozaki, N. *Hydrobiologia* **1999**, *394*, 129−144.
(33) Takahashi, T.; Sutherland, S. C.; Sweeney, C.; Poisson, A.; Metzl, N.; Tilbrook, B.; Bates, N.; Wanninkhof, R.; Feely, R. A.; Sabine, C.; Olafsson, J.; Nojiri, Y. *Deep-Sea Res. II* **2002**, *49*, 1601−1622.

Table 2. Summary of SAMI-pH Performance Characteristics

performance criteria	description	result
relative accuracy	agreement between the UV−visible and SAMI-pH	-0.003 ± 0.004 pH unit
precision	reproducibility for a single sample (borate buffer pH 8.01)	better than ± 0.005 pH unit
dynamic range	the working range of the indicator (determined assuming an absorbance minimum of 0.1 and a maximum indicator concentration of 6.5×10^{-6} M, at 10 °C)	7.61−8.73 pH units
response time	time required to detect 99% of a pH change	∼5 min
flush time	time required to completely flush the indicator from the plumbing	∼6 min
indicator consumption	assuming 48 measurements per day at 50 μL per pH measurement cycle	73 mL of 2.00×10^{-2} mol kg^{-1} CR month^{-1}
battery power	the length of deployment (18 D-cells, 16 C-cells; assuming 2 measurement cycles/h)	∼1 month

studies require absolute pH accuracy of at least 0.005 pH unit.[34] Although this level of accuracy is readily achieved with the SAMI-pH relative to the UV−visible spectrophotometer uncertainty in the pK_a' (eq 2), is a more significant problem. The ionic strength and temperature dependence of indicator pK_a' must be accurately quantified[15,22,23] and, for deep water measurements, the pressure dependence.[35] The present pK_a' was determined using low ionic strength buffers and has an uncertainty of ± 0.05 due to the uncertainty of extrapolating to the ionic strength of the river water.[23] However, pK_a''s at seawater ionic strengths are known to $< \pm 0.004$.[16]

CONCLUSIONS

The SAMI-pH utilizes a simple pump and plumbing design to achieve performance comparable to our laboratory-based spectrophotometric pH measurements. Excellent stability is obtained through periodic blank measurements, use of an absorbance ratio for calculation of pH and a simple, robust spectrograph-based detection system. As we explained earlier,[30] a response based on an absorbance ratio can provide long-term calibration-free measurements. In optical chemical sensors that utilize an indicator reaction with two absorbing species in equilibrium (e.g., complexed/uncomplexed or protonated/deprotonated), the absorbance ratio-based response (the right side of eq 2) will depend only upon the solution equilibrium. In other words, the absorbance ratio-based response is fixed by the thermodynamic variables temperature, pressure, concentration, and ionic strength. An important consequence is that all sensors should have an identical response (i.e., the same absorbance ratio) for the same thermodynamic conditions and this response should not change with time, assuming good photometric and wavelength accuracy and stability. More extensive field testing of the SAMI-pH is required to fully verify these predictions, ideally a prolonged period (3−6 months) that would include a larger and more dynamic pH and alkalinity range than found in the present field study.

Table 2 summarizes the most important features of the SAMI-pH. The instrument's characteristics include a precision of $\leq \pm 0.005$, good long-term stability, low power, minimal indicator usage, and relatively rapid response time (∼5 min for 99% response). These features make the SAMI-pH amenable for many autonomous sensing applications. In cases where a faster response time is required, sample throughput can be increased by further reduction of the plumbing flush volume. Shorter analysis time would also significantly reduce the power requirements.

The pH perturbation and large spectral band-pass are complicating factors, which could be improved in future designs. By increasing the optical path length, indicator concentration can be reduced, thus lessening indicator perturbation effects. Liquid core waveguides (LCWs) offer the possibility of long path lengths with minimum flush volume and high light throughput. LCWs have recently been used in absorbance[36] as well as luminescence[37] instruments with path lengths exceeding 10 cm. Further improvement in the light throughput (e.g., use of a higher intensity lamp) would make it possible to use smaller detectors, subsequently reducing the band-pass. Because SAMI-pH performance is currently near the limit of the precision required for CO_2 carbon cycle calculations,[34] these changes are only viable if they do not compromise the data quality achieved with the present system.

(34) Millero, F. J. *Geochim. Cosmochim. Acta* **1995**, *59*, 661−677.
(35) Hopkins, A. E.; Sell, K. S.; Soli, A. L.; Byrne, R. H. *Mar. Chem.* **2000**, *71*, 103−109.
(36) Byrne, R. H.; Liu, X.; Kaltenbacher, E. A.; Sell, K. *Anal. Chim. Acta* **2002**, *451*, 221−229.
(37) Li, J.; Dasgupta, P. K. *Anal. Chim. Acta* **2001**, *442*, 63−70.

ACKNOWLEDGMENT

We thank Terry Hammar (Woods Hole Oceanographic Institution) for providing technical assistance. This work was supported through grants from the National Science Foundation Ocean Sciences (OCE 9812513) and Office of Naval Research (N00014-00-1-0573).

Received for review September 12, 2002. Accepted January 15, 2003.

AC020568L